

Retraction

Retracted: Radio Frequency Link and User Selection Algorithm for 5G Mobile Communication System

Complexity

Received 23 January 2024; Accepted 23 January 2024; Published 24 January 2024

Copyright © 2024 Complexity. This is an open access article distributed under the Creative Commons Attribution License, which permits unrestricted use, distribution, and reproduction in any medium, provided the original work is properly cited.

This article has been retracted by Hindawi following an investigation undertaken by the publisher [1]. This investigation has uncovered evidence of one or more of the following indicators of systematic manipulation of the publication process:

- (1) Discrepancies in scope
- (2) Discrepancies in the description of the research reported
- (3) Discrepancies between the availability of data and the research described
- (4) Inappropriate citations
- (5) Incoherent, meaningless and/or irrelevant content included in the article
- (6) Manipulated or compromised peer review

The presence of these indicators undermines our confidence in the integrity of the article's content and we cannot, therefore, vouch for its reliability. Please note that this notice is intended solely to alert readers that the content of this article is unreliable. We have not investigated whether authors were aware of or involved in the systematic manipulation of the publication process.

Wiley and Hindawi regrets that the usual quality checks did not identify these issues before publication and have since put additional measures in place to safeguard research integrity.

We wish to credit our own Research Integrity and Research Publishing teams and anonymous and named external researchers and research integrity experts for contributing to this investigation.

The corresponding author, as the representative of all authors, has been given the opportunity to register their agreement or disagreement to this retraction. We have kept a record of any response received.

References

- [1] Z. Lv and Z. Xi, "Radio Frequency Link and User Selection Algorithm for 5G Mobile Communication System," *Complexity*, vol. 2021, Article ID 1976499, 10 pages, 2021.

Research Article

Radio Frequency Link and User Selection Algorithm for 5G Mobile Communication System

Zhengen Lv¹ and Zhenghao Xi² 

¹Potevio Information Technology Co., Ltd, Beijing 100080, China

²School of Electronic and Electrical Engineering, Shanghai University of Engineering Science, Shanghai 201620, China

Correspondence should be addressed to Zhenghao Xi; zhenghaoxi@hotmail.com

Received 9 April 2021; Revised 29 April 2021; Accepted 5 May 2021; Published 14 June 2021

Academic Editor: Zhihan Lv

Copyright © 2021 Zhengen Lv and Zhenghao Xi. This is an open access article distributed under the Creative Commons Attribution License, which permits unrestricted use, distribution, and reproduction in any medium, provided the original work is properly cited.

Based on the millimetre-wave time-domain channel detector, this paper conducts channel measurement and modelling for different scenarios and antenna types in typical frequency bands and thus carries out a study on the propagation characteristics of millimetre-wave channels in typical frequency bands and scenarios for 5G. The time-varying characteristics and modelling methods of millimetre-wave clusters are studied, and the time-varying channel simulation strategy and linear regression fitting method are used to establish the time-varying generation and extinction model of clusters by combining the measured data of 26 GHz large-scale antenna channels. The algorithm is based on the correlation dictionary and achieves the efficient and optimal selection of large-scale antenna arrays in the millimetre-wave band. A low-complexity multiuser hybrid precoding design scheme is proposed based on the wideband millimetre-wave large-scale Multiple-Input Multiple-Output (MIMO) system. The scheme aims to maximize the system spectral efficiency and introduces the net spectral efficiency as a bridge to decouple the analogy precoding design from the digital precoding design, thus significantly reducing the computational complexity. In the analogy precoding stage, a Hungarian algorithm-based beam assignment method is proposed to avoid beam conflicts and maximize the net spectral efficiency of the system; in the digital precoding stage, the equivalent channel matrix of each subcarrier is diagonalized to eliminate multiuser interference. Finally, the effectiveness of the scheme is verified by simulation. In this paper, we focus on the radio frequency (RF) link and user selection algorithm of 5G mobile communication system. Through the study of these two aspects, the RF link of our communication system has high stability and reliability, and through the study of the algorithm used for selection, our results also have a strong practical value.

1. Introduction

As the global mobile communication technology continues to develop rapidly, new applications and new demands such as ultra-high-definition video services, mobile cloud computing, and high-quality data services are emerging, and mobile communication technology is facing higher and higher challenges. To meet the demand for high-quality mobile data services, the research and application breakthrough of 5G mobile communication technology is imminent [1]. Four typical application scenarios of 5G are continuous wide area coverage, low power consumption and large links, low latency, high reliability, and high capacity hotspots. The application of continuous wide-area coverage

technology allows users to experience reliable high-speed services and continuous access to the network even in the case of high-speed mobile, with the main goal of 100-megabit rate user experience [2]. Dense areas are the main application sites for high-capacity hotspots, which mainly include dense offices, stadiums, open-air concerts, and so on. High-capacity hotspots can provide high-speed data services to many users in a short period to meet their business needs. The user experience rate, peak rate, and traffic density requirements can reach 1 Gbps, tens of Gbps, and tens of Tbps/km, respectively [3]. Driverless driving is the main application scenario of low latency and high reliability of the Internet of Vehicles. Such scenarios have extremely high requirements on latency, transmission, and retransmission

probability and need to meet ms-level latency. The low-power large connection scenario is mainly for data collection and sensing as the goal of the application scenario, with small packets, low power consumption, mass connection, and other characteristics [4].

With the increasing scarcity of spectrum resources, the millimetre-wave band is the primary choice for 5G communication systems because of the huge space for spectrum exploitation. Millimetre-wave is an electromagnetic wave with a spectrum between 30 GHz and 300 GHz and a wavelength between 1 and 10 mm, which is very wide and short [5]. Therefore, millimetre waves have a large path loss when propagating in free space, and because of the use of the high-frequency band for communication, the transmission distance will be shortened and the coverage capability will be greatly reduced, which requires more base stations to maintain the transmission capability. The good thing is that the millimetre-wave wavelength is very short, so the antenna can be significantly reduced. Even if the number of antennas can increase, the number of base stations that can be established is very small. 5G can use microbase stations instead of macrobase stations, and then, 4G base stations will be much more. These are large-scale multiple-input multiple-output technologies [6]. In a large-scale MIMO system, there are many transmitting and receiving antennas, so the transmitter can send signals through many antennas, while the receiver can receive signals through multiple antennas, thus achieving a significant improvement in communication quality. Reducing the waste of space resources is a major advantage of large-scale MIMO; with multiple antennas transmitting and receiving, the channel capacity can be significantly increased without increasing the antenna transmission power and spectrum resources. Large-scale MIMO has many antennas, and if each antenna is linked to a separate RF chain as in traditional MIMO, then the hardware cost and complexity will increase significantly.

This paper focuses on the multiuser hybrid precoding technique for millimetre-wave massive MIMO systems. This paper investigates the narrowband millimetre-wave channel and broadband millimetre-wave channel models and discusses the hybrid precoding architecture for millimetre-wave massive MIMO systems. Section 1 is the introduction, which first introduces the status of millimetre-wave massive MIMO technology in 5G communication system and the importance of precoding technology in the research of millimetre-wave massive MIMO technology, to show the research background and significance of this paper, and also explains the research structure of this paper [7]. Section 2 analyses the related research in this paper; it mainly analyses the related research at home and abroad and its shortcomings and briefly explains the research in this paper. Section 3 investigates the multiuser hybrid precoding design based on the narrowband millimetre-wave large-scale MIMO system. In the beam training stage, a beam training scheme based on interval scanning is first proposed to reduce the beam training overhead; then, a beam training scheme based on selection probability is proposed to improve the flexibility of beam training. Section 4 shows system simulations through three dimensions: system model,

algorithm simulation, and performance analysis to verify the effectiveness of the proposed multiuser hybrid precoding design scheme in wideband millimetre-wave large-scale MIMO systems. Section 5 summarizes the full-text work and provides analysis and outlook of the subsequent work.

2. Related Work

MIMO technology has been extensively studied and implemented in 5G mobile communication systems [8]. By increasing the number of antennas at the transmitter and receiver ends, they can significantly improve the channel capacity and the quality of the wireless system. Initially, research focused on point-to-point MIMO systems, but point-to-point communication has many limitations, so multiuser MIMO has become a hot research topic. Multiuser MIMO installs many antennas at the base station, allowing the base station to communicate with multiple users at the same time [9]. The limitation of current multiuser multiple-input multiple-output (MU-MIMO) systems is that the base station is usually equipped with a small number of antennas. Among the antenna selection algorithms, the exhaustive enumeration algorithm is one of the best and most widely known methods. However, the exhaustive algorithm needs to calculate all combinations once, so the complexity is high, and the problem can be solved by sacrificing part of the performance for the suboptimal antenna selection algorithm with low complexity. In the literature, BER-oriented selection criteria studied for a specific selection algorithm for real receivers [10]. The literature mentions suboptimal greedy algorithms as well as the use of the branch-and-bound method for antenna selection with the best results [11]. Most of these algorithms search for antennas after many calculations as well as iterations to get better results by increasing the complexity, but when the number of antennas becomes large, it inevitably increases the search time [12]. In applying the antenna selection algorithm, we have done some research on how to reduce the RF chain switching as well as channel estimation. One of the purposes of antenna selection is to reduce the hardware cost and power consumption, and if a full array of switches is used, then many antennas will incur a high overhead [13]. Therefore, there are an increasing number of studies on how to reduce the number of antenna switches. The literature mentions the use of subantenna arrays, where each RF chain is connected to a disjoint subarray of the same size, and the same number of antennas is selected from each subarray [14].

To solve the problems of high cost and high power consumption of RF links for digital precoding and poor performance of analogy precoding, a hybrid precoding scheme combining analogy precoding and digital precoding schemes was proposed in the literature [15]. The hybrid precoding scheme contains a low-dimensional digital precoding matrix and a high-dimensional analogy precoding matrix connected by a very small number of RF links. The hybrid precoding scheme can effectively reduce the hardware cost and power consumption of the system, and its performance is close to the optimal pure digital precoding. There are two types of hybrid precoding schemes in use,

namely, fully connected hybrid precoding schemes and partially connected hybrid precoding schemes. Based on this, literature proposed a hybrid precoding algorithm based on the sparse characteristics of the millimetre-wave channel and an orthogonal matching tracking method based on the optimization of the system reachability and rate, which can approach the performance of pure digital precoding, but it needs to know in advance the millimetre-wave channel [16]. The literature proposes a low-complexity hybrid precoding scheme based on the antenna array response corresponding to the maximum gain path of the millimetre-wave as the analogy precoding, and the digital precoding part uses the RZF precoding scheme, which has a reduced performance compared with the optimal digital precoding scheme, but hardware complexity and power consumption are lower [17].

Millimetre-wave massive MIMO systems have the advantages and disadvantages of conventional massive MIMO systems but also face great challenges in terms of precoding technology due to the use of higher frequency band millimetre-wave carriers. If the system still uses the traditional purely digital precoding technology, this makes it extremely difficult to implement in the actual system. As the number of antennas increases, each antenna also needs to connect the corresponding RF link, its power consumption and hardware costs will also increase, and the possibility of implementation is extremely small. If the system adopts an analogy precoding technique, the system performance is proportional to the number of beams because the analogy precoding technique is limited by the number of analogy beams, but the system overhead also increases. Therefore, combining the advantages of both precoding techniques, a hybrid precoding technique using a combination of analogy/digital precoding techniques is proposed, which enables the system performance to be effectively improved by using a limited number of RF links to connect a large number of antennas and a large number of phase shifters in between to achieve space-division multiplexing of the beams. The current base station antenna architectures for millimetre-wave massive MIMO systems are fully connected millimetre-wave massive MIMO systems and partially connected millimetre-wave massive MIMO systems.

3. 5G Mobile Communication System RF Link and User Selection Algorithm Research

3.1. Millimetre-Wave Massive MIMO System Model. The downlink data transmission of a multiuser narrowband millimetre-wave massive MIMO system is considered, and its system transmission model is shown in Figure 1. The base station adopts a hybrid precoding structure with N_s data streams, N_{RF} links, and N_{BS} root ULA antennas ($1 \leq N_s \leq N_{RF} \leq N_{BS}$); each user is equipped with a single RF link and N_{UE} root ULA antenna using an analogy merged architecture. Since the users are equipped with a single RF link, the base station communicates with each user over a single data stream. The number of users that can be served simultaneously by the base station K is equal to the number of data streams N_s at the base station and is limited by the

number of RF links N_{RF} at the base station; that is, $K = N_s \leq N_{RF}$. It is usually assumed that the number of simultaneous users served by the base station is the same as the number of RF links of the base station; that is, $K = N_{RF}$, and if $K < N_{RF}$, the base station will use K RF links to serve K users and turn off $(N_{RF} - K)$ RF links to save energy consumption.

In downlink data transmission, the signal k s received by the k -th user is expressed as (1), where $s = [s_1, s_2, \dots, s_k]^T$ denotes the data symbol vector, which obeys the total transmit power PDL constraint:

$$y_k = w_k^H H_k^{NB,DL} F_{RF} F_{BB} s - w_k^H n_k^{DL}. \quad (1)$$

In a narrowband millimetre-wave massive MIMO system, based on the SV channel model, the channel matrix between the base station and the k -th user is expressed as (2), where L_k denotes the number of multipath between the base station and the k -th user, a_l , k denotes the complex gain of the l -th path, and $\phi_{l,k}$ and $\theta_{l,k}^2$, k denote the N_{UE} and N_{BU} of the l -th path, respectively.

$$H_k^{NB,DL} = \sqrt{\frac{N_{BU} N_{UE}}{L_k}} \sum_{l=1}^{L_k} a_{l,k} a(N_{UE}, \theta_{l,k}^2) a_k^H(N_{BU}, \phi_{l,k}, \theta_{l,k}^2). \quad (2)$$

The received signal strength gradually decreases as the distance between the transmitter and receiver increases, and the path loss model is used to describe the variation law of signal strength with the transmitting and receiving distance [18]. In the simulation and design of mobile communication systems, a reasonably large-scale path loss model and shadow effect model can help predict and analyse the coverage and interference accurately. Antennas with certain gain are used at both transceiver and transmitter, and the measurement system contains the amplifier and low-noise amplifier devices as well as link gain. To obtain the actual propagation channel, the additional gain needs to be stripped from the measurement data. In (3), G_t is the transmit antenna gain, G_r is the receive antenna gain, G_{PA} is the amplifier gain, G_{LANA} is the gain of the low-noise amplifier, and G_{LME} is the link gain.

$$P = \frac{100}{e} \ln \left\{ \sum h(\tau)^2 \right\} + G_t + G_r - G_{PA} + G_{LANA} - G_{LME}. \quad (3)$$

To compare different multipath channels and to provide guidance for wireless system design, angular expansion is used as an important parameter to describe the spatial dispersion of the channel. The root-mean-square angular expansion is defined as the square root of the second-order central moment of the angular power spectrum. However, in practice, to avoid the effects due to the cyclic periodicity of the angle, the cyclic angle expansion is generally utilized instead of the root-mean-square angle expansion. In the 3GPPSCM channel model, the cyclic angular expansion is a constant that does not change due to angular offset. For the case of N multipaths with M subparts within each multipath, the angle expansion is calculated as follows:

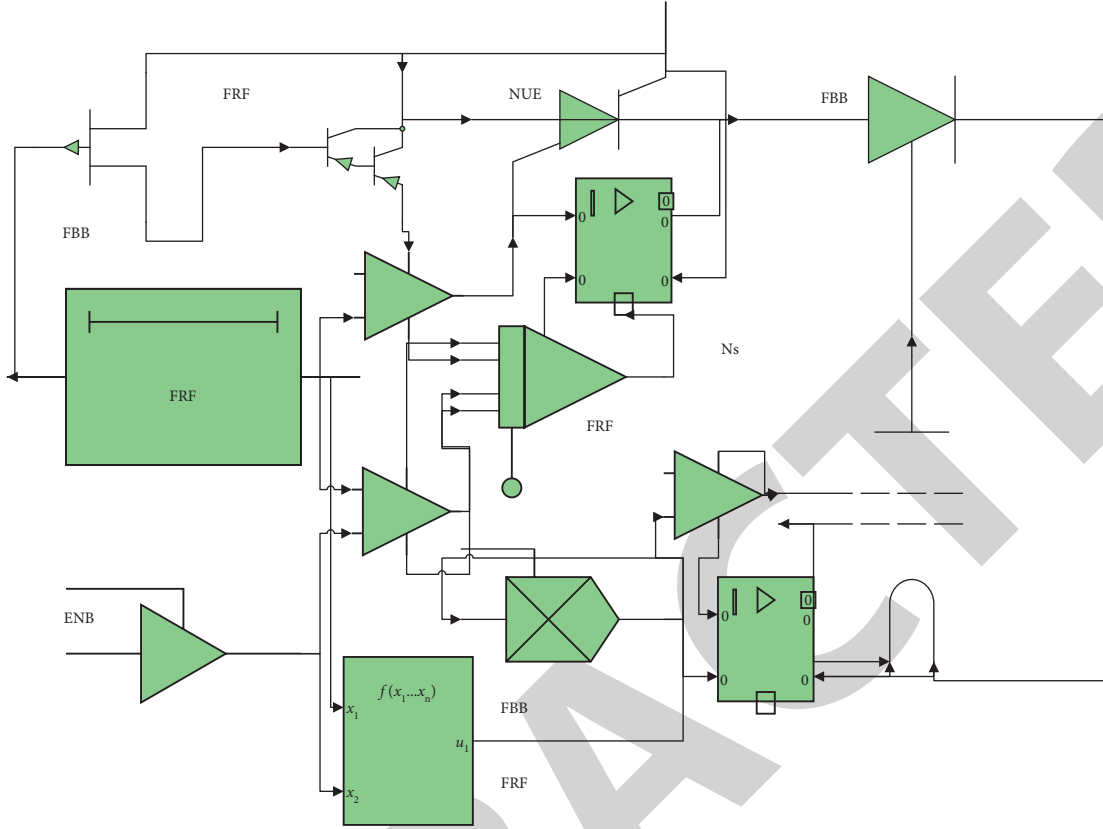


FIGURE 1: The hardware circuit diagram in the transmission model of the MIMO system.

$$\sigma_{AS} = \sqrt{\frac{\sum_{m=1}^M \sum_{n=1}^N (\theta_{n,m,\mu})^2 P_{m,n}}{\sum_{m=1}^M \sum_{n=1}^N P_{m,n}^2}} \quad (4)$$

3.2. RF Link and User Selection Algorithm Based on User Waiting Queue. Antenna selection is a key technology in large-scale MIMO, which uses RF switches instead of phase shifters to greatly reduce the number of RF chains and hardware complexity, and therefore has a unique advantage in MIMO systems. The antenna selection process needs to select the appropriate antenna based on the channel state information, so it also brings an important problem for antenna selection. Large-scale MIMO requires a large number of antennas for signal transmission. It is very difficult to select some of the appropriate antennas from a large number of antennas. The complexity of using algorithms such as exhaustive method is very high. The problem of how to use a low-complexity antenna selection method to select the appropriate antenna needs to be considered [19].

The probability of a base station serving all K users without any beam conflict is equal to the probability of selecting K mutually dissimilar base station code words from N_{BS} base station code words, which is denoted as

$$P_{NC} = \frac{N_{BS}^2!}{N_{BS}^2 (N_{BS}^2 + K)!} \quad (5)$$

Since the distribution of users in space is random, the N_{BS}^2 beams formed by the base station code word in different directions cannot be precisely directed to the users, thus causing channel energy leakage. The relationship between the response vector of the downlink channel $C(n)$ and the base station code word can be expressed as

$$C(n) = |a_k^H(N_{BS}^2, \varphi) f_c(n)|^2 \quad (6)$$

Define the virtual channel matrix expressed as (7). In the absence of channel noise, H_k^v and N_{UE} are identical; that is, H_k^v is the measured value of w_k^H obtained by beam training, so the equivalent channel gain is the same as the maximized virtual channel gain.

$$H_k^v = w_k^H n_k^{DL} N_{UE} \theta_{l,k}^2 \quad (7)$$

Figure 2 represents the schematic of the virtual channel gain distribution when $N_{BS} = 64$ and $N_{UE} = 64$, where x -axis and y -axis represent the rows and columns of the virtual channel matrix, respectively, and the z -axis represents the magnitude of the virtual channel gain. As can be seen from Figure 2, the channel has three paths, each of which will have a peak, and the elements with relatively small virtual channel gain are distributed around the peak, characterizing the leakage phenomenon of channel energy around the peak. The energy of each channel path is mainly concentrated at the intersection of two adjacent rows and two adjacent columns of the virtual channel matrix, and the

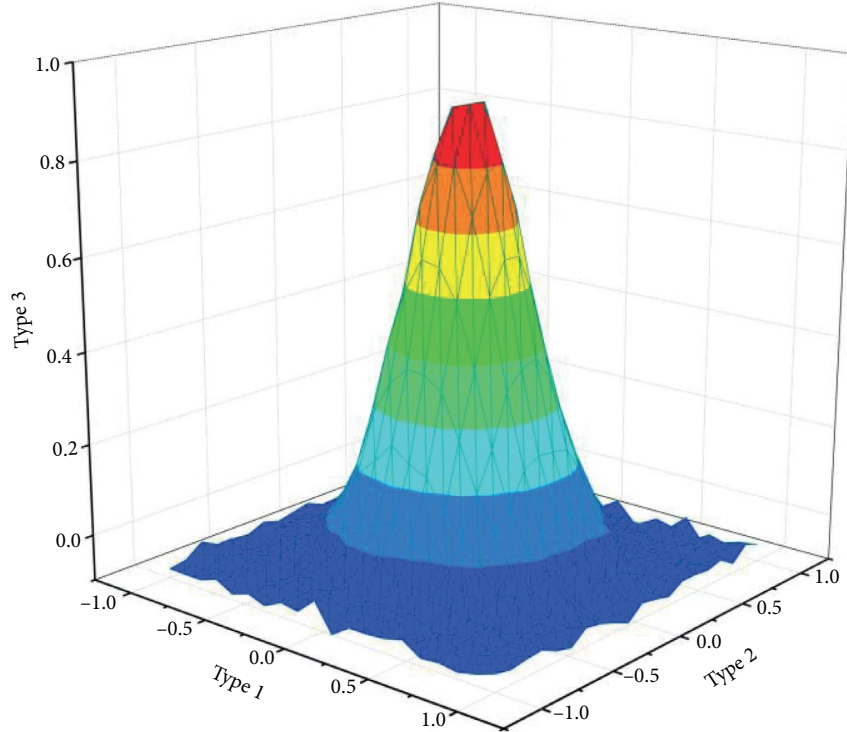


FIGURE 2: Virtual channel gain distribution diagram.

peak must be in one of the four intersection points. Since there is energy leakage in the channel, there are multiple beams with higher virtual channel gain between the base station and each user that can be used as a candidate beam set, which inspires us to avoid the beam conflict problem by a suitable beam assignment algorithm.

In the design phase of analogy precoding and analogy merging, to avoid beam conflict, (7) needs to be reconstructed as follows:

$$\begin{aligned} f_i^{\text{RF}} &= f_j^{\text{RF}} n_k^{\text{DL}}, \\ \sum_{n=1}^N (\theta_{n,m,\mu})_m^2 &= \text{NB}_{\text{BS}}^2 (\text{NB}_{\text{BS}}^2 + K). \end{aligned} \quad (8)$$

3.3. Hybrid Precoding Hierarchical Design Based on Wideband Channels. In the design of hybrid precoding based on wideband millimetre-wave channel, the equivalent channel gain distribution of different base station code words on different Orthogonal Frequency Division Multiplexing (OFDM) subcarriers is different, so the beam allocation method based on equivalent channel gain in the narrowband millimetre-wave channel cannot be applied to wideband millimetre-wave channel scenario. As a result, it is not feasible to decouple the analogy precoding and digital precoding design by introducing only equivalent channel gain. Therefore, it is not feasible to decouple the analogy precoding and digital precoding design by introducing only the equivalent channel gain, and how to allocate the beam for all users in the analogy precoding design phase is the

biggest challenge for the hybrid precoding design based on wideband millimetre-wave channels. Based on the net spectral efficiency of the system, the analogy precoding can be decoupled from the digital precoding [20]. As shown in Figure 3, the system's net spectral efficiency is the sum of the spectral efficiencies of all users in multiple single-user scenarios without considering multiuser interference. In the analogy precoding design, the optimization problem of a single multiuser scenario is transformed into a joint optimization problem of multiple single-user scenarios.

There are many types of user services, three of which are listed here: video playback, instant messaging, and web requests [21–25]. Users have different requirements for different service types, and two characteristics are listed here: immediacy requirement and data volume per request. Table 1 describes the differences in these two characteristics among the three service types. From Table 1, there are significant differences in the immediacy and data-per-arrival requirements, which will have a significant impact on the performance of the algorithm, and therefore should be differentiated by the user's business type.

4. Analysis of Results

4.1. User Selection Algorithm Validity Analysis. To verify the effectiveness of the proposed algorithm, this section simulates and analyzes the proposed algorithm under different signal-to-noise ratios and a different number of receive antennas and compares it with the all-digital optimal performance algorithm and the proposed partially connected hybrid precoding SIC algorithm and the fully connected hybrid precoding LUM algorithm, respectively. The

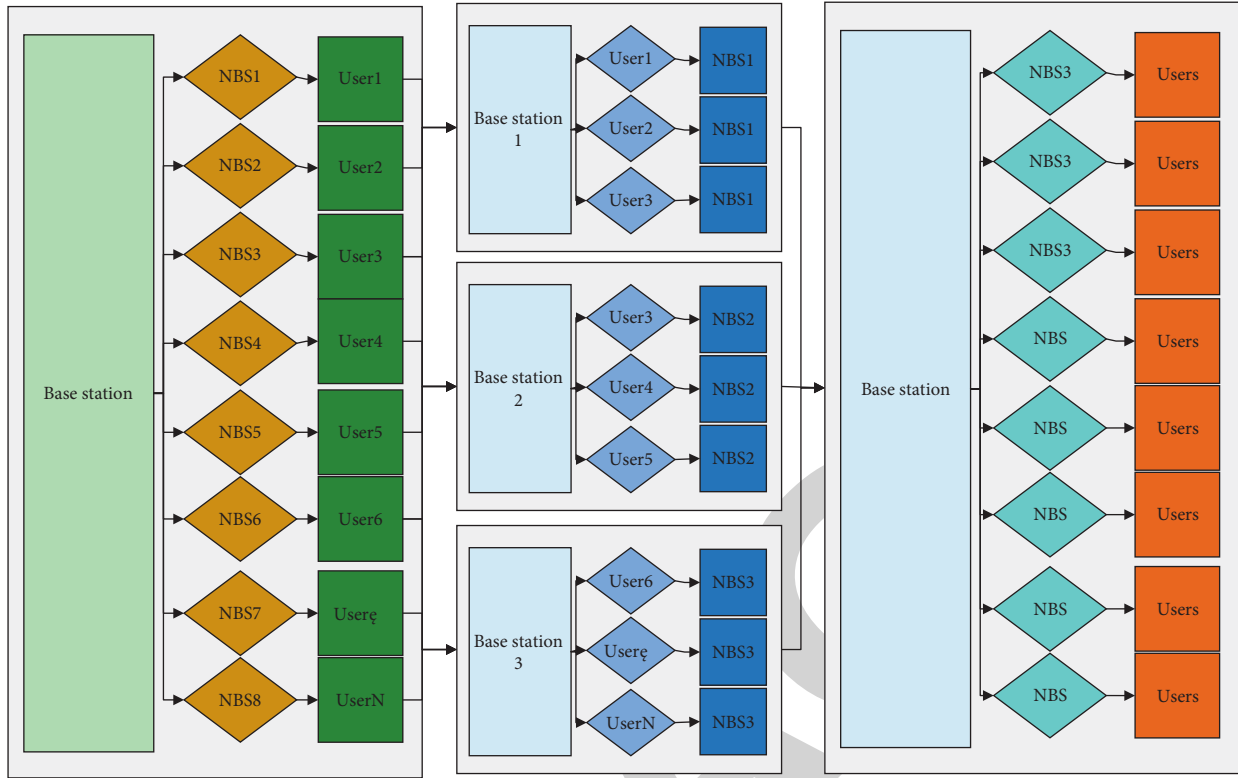


FIGURE 3: Illustration of the physical meaning of net spectral efficiency.

TABLE 1: Differences between the three business types.

Demand type	Immediacy	Data volume per arrival
1	6	19
2	14	19
3	6	11
4	18	8
5	5	7
6	10	7
7	10	13
8	14	14
9	8	14
10	19	5

comparison of system reachability and rate is shown in Figure 4 for $N \times K = 64$, NRF=8 millimetre-wave massive MIMO system. As the number of antennas increases, the reachable and rate of the system increases accordingly, and the performance of the BM-SIC algorithm is significantly better than that of the SIC algorithm. The proposed BM-SIC algorithm is based on a partially connected millimetre-wave large-scale MIMO system, and its performance is generally lower than that of the fully connected scheme, but the hardware complexity is much lower than that of the fully connected hybrid preprogramming scheme, as shown in Figure 4.

Figure 5 shows the system reachability and rate versus the number of receiving antennas for a millimetre-wave large-scale MIMO system with $N = 128$ and SNR=0 dB. In this figure, the system reachability and rate increase continuously with the number of receiving antennas, and the

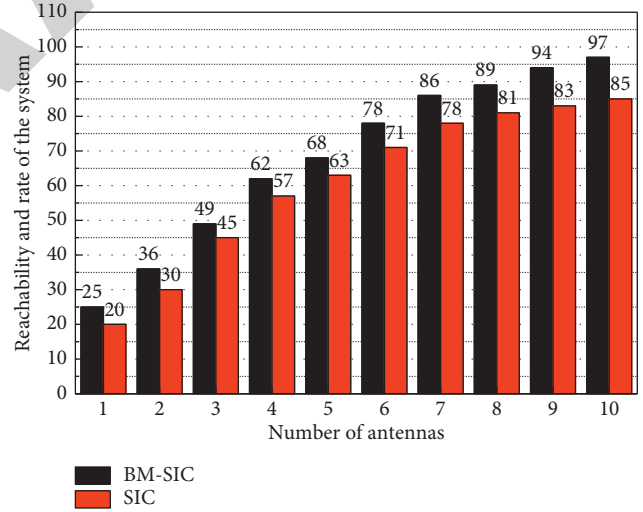


FIGURE 4: Average system reaches and rate comparison.

proposed BM-SIC algorithm outperforms the LUM algorithm as the number of receiving antennas increases, and the running rate of the proposed algorithm is slightly lower than that of the fully connected hybrid precoding and fully digital precoding schemes and can reach about 80% of the fully digital precoding.

The band-based matrix precoding scheme is based on predesigning the digital precoding matrix at the base station side as a band matrix and determining the final analog precoding matrix and digital precoding matrix with the system reachability and rate as the objective function. The

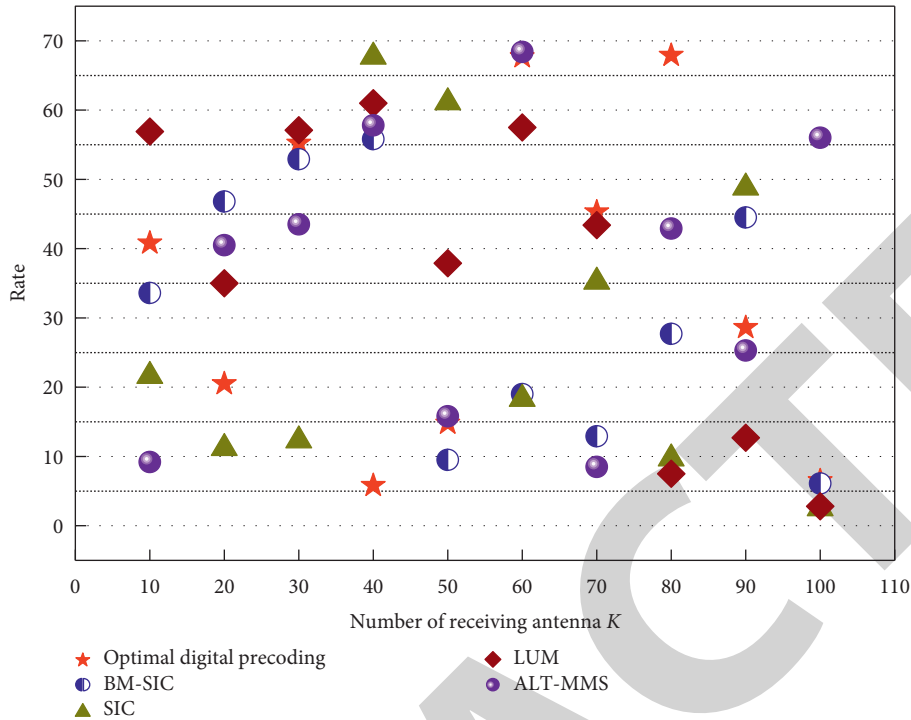


FIGURE 5: System reaches and rate vs. the number of receiving antennas.

Boyer–Moore Successive Interference Cancellation (BM-SIC) algorithm scheme is compared with the all-digital precoding scheme and other algorithm schemes in various cases. Simulation results show that the BM-SIC algorithm system reachability and rate are better than the SIC-based algorithm scheme and avoids the disadvantage of the SIC algorithm in that the number of RF links is equal to the transmitted data stream and has fewer limitations.

4.2. Simulation Analysis of User Selection Algorithm.

Figure 6 shows the channel capacity comparison between the proposed hybrid precoding algorithm and the existing precoding methods for $NT = 64$, $N_r = 16$, and $N_s = 4$ concerning the RF chain. When $N_s = 2$ and RF chain is less than 5, the proposed precoding algorithm works better than the Space Oblique Mercator Projection (SOMP) algorithm. As the RF chain increases, the proposed precoding algorithm gradually approaches the optimal unconstrained precoding, and finally, it is almost the same as the optimal unconstrained precoding. In Figure 6, we can visualize the data with $NT = 64$, $N_r = 16$, and $N_s = 4$. We can see that the results are better in the case of $NT = 64$ and the worst in the case of $N_r = 4$. This should also show that the higher the number of N , the better the results.

The previously mentioned simulation proves that the performance of the hybrid precoding algorithm proposed in this paper is basically the same as that of the SOMP algorithm, and the precoding/combination matrix can be obtained directly without complex iterations, which has a great advantage in terms of algorithm complexity. The feasibility of the antenna selection algorithm approach combining hybrid precoding is verified in the following. Figure 7

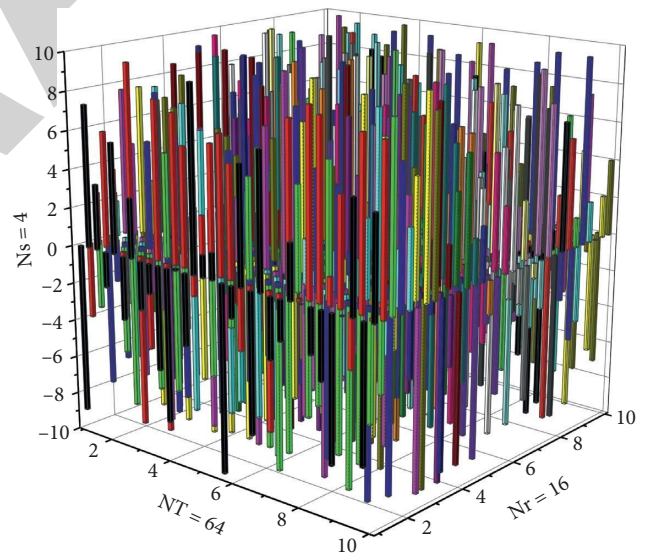


FIGURE 6: Spectral efficiency vs. RF link in millimetre-wave MIMO systems.

illustrates the relationship between the number of antennas and the channel capacity at the same SNR. It can be observed that the hybrid precoding is constant when the number of antennas increases, while the antenna selection algorithm combined with hybrid precoding increases the spectral efficiency as the number of antennas increases. The spectral efficiency is the same as the corresponding hybrid precoding when the number of selected antennas reaches the maximum. It can also be observed that the proposed antenna selection algorithm combined with hybrid precoding is only

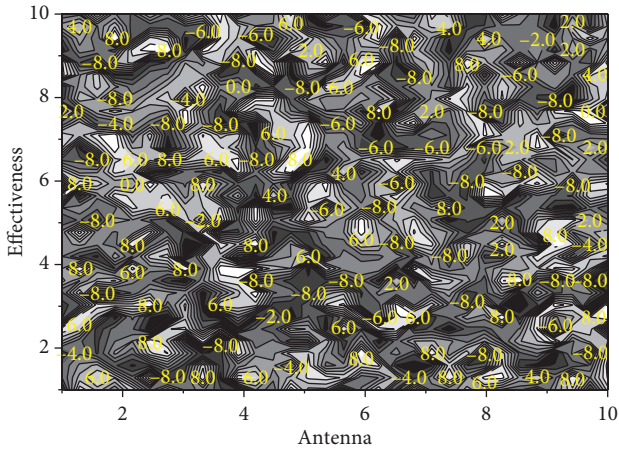


FIGURE 7: Spectral efficiency vs. the number of antennas in a 16×16 mm wave MIMO system.

about 1.5 bit/s/Hz less than the optimal unconstrained precoding method when two antennas are selected, and it is getting closer. The performance is the same as that of hybrid precoding when the number of selected antennas is greater than 10.

The simulation is compared and it is shown that the algorithm is the same as the SOMP algorithm and has a lower complexity. Next, an antenna selection algorithm combining hybrid precoding is proposed, which first uses the optimal unconstrained precoding to find the antenna selection matrix, then uses this matrix as the basis to obtain the equivalent channel, and finally uses the low-complexity hybrid precoding algorithm proposed in this chapter to solve the hybrid precoding matrix/combined matrix. The results show that the antenna selection algorithm using a combination of hybrid precoding can transmit signals using partial antennas with little loss of spectral efficiency.

4.3. User Selection Algorithm Performance Analysis.

Figure 8 compares the simulation runtimes of different precoding schemes for a different number of user's K . The simulations are based on MATLAB R2014b software for a desktop computer with four 3.6 GHz Intel Core i5-3470 CPUs and 8 GB of RAM. The simulation results show that the simulation runtime of all precoding schemes increases with the number of users K . The all-digital precoding scheme has the fastest simulation runtime among all precoding schemes, but it is difficult to implement all-digital precoding in large-scale MIMO systems in practical engineering. The simulation runtime of the proposed hybrid precoding scheme is much faster than that of the SOMP hybrid precoding scheme because the SOMP hybrid precoding scheme requires repeated iterations in solving the analogy and digital precoding matrices, resulting in many operations, while the proposed hybrid precoding is mainly focused on the Hungarian algorithm in beam assignment. The simulation run time of the proposed hybrid precoding scheme is slightly slower than that of the TS hybrid precoding scheme because, unlike the proposed hybrid

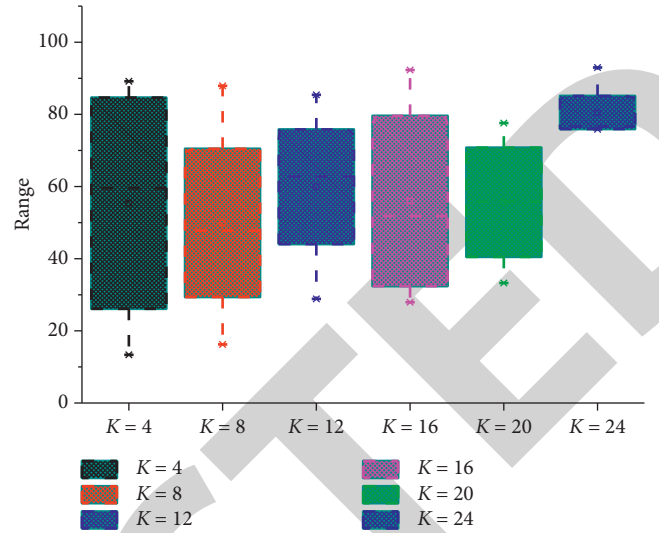


FIGURE 8: Simulation runtime comparison.

precoding scheme, the TS hybrid precoding scheme allocates the beam with the largest equivalent channel gain to each user in the analogy precoding design and does not use the beam allocation algorithm, which requires a certain number of operations, to resolve the beam conflicts.

Figure 9 shows the system proposed algorithm considering the system reachability and rate of quantizer using 1-bit DACs versus the signal-to-noise ratio. From the figure, it can be seen that the use of 1-bit DACs makes the system performance deficit more serious; with the increase of signal-to-noise ratio, the system reachability and rate of the algorithm using 1-bit DACs tends to level off, which is due to the presence of a larger quantization noise, making the performance loss significant. However, its hardware cost and power consumption are relatively lower. To improve the system performance, DACs can be quantized with multiple bits.

The band-based matrix precoding scheme is based on predesigning the digital precoding matrix at the base station side as a band matrix and determining the final analogy precoding matrix and digital precoding matrix with the system reachability and rate as the objective function. The BM-SIC algorithm scheme is compared with the all-digital precoding scheme and other algorithm schemes in various cases. Simulation results show that the BM-SIC algorithm system reachability and rate is better than the SIC-based algorithm scheme and avoids the drawback of an equal number of RF links to the transmitted data stream of the SIC algorithm, which is less limited. The minimum error-based hybrid precoding scheme splits the optimal all-digital and equivalent hybrid precoding matrices based on the block diagonalization property of the analogy precoding matrix and obtains the analogy and digital precoding vectors corresponding to each RF link in turn. First, the optimal analogy precoding matrix and digital precoding matrix are obtained without considering the phase accuracy; second, the optimal analogy precoding matrix and digital precoding matrix of the algorithm are obtained with limited phase accuracy of the phase shifter; finally, the system performance

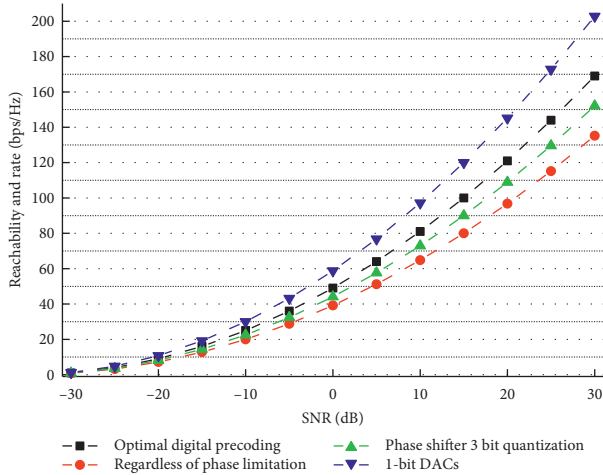


FIGURE 9: Algorithm performance comparison results.

of the MDM algorithm in the case of 1-bit DACs is also considered in the simulation. The performance of the MDM algorithm in the 1-bit DACs case is also considered in the simulation. The simulation results show that the MDM algorithm can outperform the performance of the SIC algorithm with lower computational complexity and no limitations.

5. Conclusion

In this paper, a low-complexity multiuser hybrid precoding design scheme is proposed based on a wideband millimetre-wave large-scale MIMO system. The scheme adopts the hierarchical design idea to maximize the system spectral efficiency as the design goal and introduces the net spectral efficiency as a bridge to decouple the analogy precoding design from the digital precoding design. In the analogy precoding stage, a beam assignment method based on the Hungarian algorithm is proposed to avoid beam conflicts and maximize the net spectral efficiency of the system; in the digital precoding stage, the equivalent channel matrix of each subcarrier is diagonalized to eliminate multiuser interference. Simulation results show that the proposed hybrid precoding scheme can effectively solve the beam conflict problem of the millimetre-wave large-scale MIMO system under the wideband channel model with lower computational complexity, and the system performance is significantly better than that of the TS and SOMP hybrid precoding schemes. As the key technology of 5G, the precoding technology of downlink for large-scale MIMO and millimetre wave technology is one of its key research directions. This paper only addresses the study of precoding techniques in partially connected millimetre-wave massive MIMO systems, while precoding techniques based on fully connected millimetre-wave massive MIMO also need to be studied. Moreover, the use of low-power, low-cost hardware to enable high performance in millimetre-wave large-scale MIMO systems is an open research problem. This paper does some research on the low complexity ZF precoding algorithm for traditional large-scale MIMO systems and the

hybrid precoding algorithm for partially connected millimetre-wave large-scale MIMO systems, but the depth of the paper needs to be improved due to the limited level of the authors and the lack of scientific research.

Data Availability

The data used to support the findings of this study are available from the corresponding author upon request.

Conflicts of Interest

The authors declare that they have no conflicts of interest.

References

- [1] H.-C. Chao, H.-H. Cho, T. K. Shih, and C.-Y. Chen, "Bacteria-inspired network for 5G mobile communication," *IEEE Network*, vol. 33, no. 4, pp. 138–145, 2019.
- [2] R. Pal, K. V. Srinivas, and A. K. Chaitanya, "A beam selection algorithm for millimeter-wave multi-user MIMO systems," *IEEE Communications Letters*, vol. 22, no. 4, pp. 852–855, 2018.
- [3] S. Sobhi-Givi, M. G. Shayesteh, and H. Kalbkhani, "Energy-efficient power allocation and user selection for mmWave-NOMA transmission in M2M communications underlying cellular heterogeneous networks," *IEEE Transactions on Vehicular Technology*, vol. 69, no. 9, pp. 9866–9881, 2020.
- [4] J. Zhang, H. Du, P. Zhang, J. Cheng, and L. Yang, "Performance analysis of 5G mobile relay systems for high-speed trains," *IEEE Journal on Selected Areas in Communications*, vol. 38, no. 12, pp. 2760–2772, 2020.
- [5] M. I. S. Mamode and T. P. Fowdur, "Survey of scheduling schemes in 5G mobile communication systems," *Journal of Electrical Engineering, Electronics, Control and Computer Science*, vol. 6, no. 2, pp. 21–30, 2020.
- [6] M. Chen, S. Lu, and Q. Liu, "Uniform regularity for a Keller-Segel-Navier-Stokes system," *Applied Mathematics Letters*, vol. 107, Article ID 106476, 2020.
- [7] Z. Kaleem, A. Ahmad, and M. H. Rehmani, "Neighbors' interference situation-aware power control scheme for dense 5G mobile communication system," *Telecommunication Systems*, vol. 67, no. 3, pp. 443–450, 2018.
- [8] H. Zhang, L. Song, and Y. J. Zhang, "Load balancing for 5G ultra-dense networks using device-to-device communications," *IEEE Transactions on Wireless Communications*, vol. 17, no. 6, pp. 4039–4050, 2018.
- [9] C. Pan, M. El-kashlan, J. Wang, J. Yuan, and L. Hanzo, "User-centric C-RAN architecture for ultra-dense 5G networks: challenges and methodologies," *IEEE Communications Magazine*, vol. 56, no. 6, pp. 14–20, 2018.
- [10] A. Y. Awan, M. Ali, M. Naeem et al., "Joint network admission control, mode assignment, and power allocation in energy harvesting aided D2D communication," *IEEE Transactions on Industrial Informatics*, vol. 16, no. 3, pp. 1914–1923, 2019.
- [11] F. L. Duarte and R. C. de Lamare, "Cloud-driven multi-way multiple-antenna relay systems: joint detection, best-user-link selection and analysis," *IEEE Transactions on Communications*, vol. 68, no. 6, pp. 3342–3354, 2020.
- [12] H. Lu, R. Proietti, G. Liu, X. Chen, and S. J. B. Yoo, "ERON: an energy-efficient and elastic RF-optical architecture for mmWave 5G radio access networks," *Journal of Optical Communications and Networking*, vol. 12, no. 7, pp. 200–216, 2020.

- [13] G. H. Sim, S. Klos, A. Asadi, A. Klein, and M. Hollick, "An online context-aware machine learning algorithm for 5G mmWave vehicular communications," *IEEE/ACM Transactions on Networking*, vol. 26, no. 6, pp. 2487–2500, 2018.
- [14] Y.-G. Lim, Y. J. Cho, M. S. Sim, Y. Kim, C.-B. Chae, and R. A. Valenzuela, "Map-based millimeter-wave channel models: an overview, data for B5G evaluation and machine learning," *IEEE Wireless Communications*, vol. 27, no. 4, pp. 54–62, 2020.
- [15] W. Zhang, Y. Wei, S. Wu, W. Meng, and W. Xiang, "Joint beam and resource allocation in 5G mmWave small cell systems," *IEEE Transactions on Vehicular Technology*, vol. 68, no. 10, pp. 10272–10277, 2019.
- [16] W. Saad, M. Bennis, and M. Chen, "A vision of 6G wireless systems: applications, trends, technologies, and open research problems," *IEEE Network*, vol. 34, no. 3, pp. 134–142, 2019.
- [17] M. A. Arfaoui, M. D. Soltani, I. Tavakkolnia et al., "Physical layer security for visible light communication systems: a survey," *IEEE Communications Surveys & Tutorials*, vol. 22, no. 3, pp. 1887–1908, 2020.
- [18] S. Savazzi, S. Sigg, F. Vicentini, S. Kianoush, and R. Findling, "On the use of stray wireless signals for sensing: a look beyond 5G for the next generation of industry," *Computer*, vol. 52, no. 7, pp. 25–36, 2019.
- [19] P. Zhang, X. Yang, J. Chen et al., "A survey of testing for 5G: solutions, opportunities, and challenges," *China Communications*, vol. 16, no. 1, pp. 69–85, 2019.
- [20] C. Fager, T. Eriksson, F. Barradas, K. Hausmair, T. Cunha, and J. C. Pedro, "Linearity and efficiency in 5G transmitters: new techniques for analyzing efficiency, linearity, and linearization in a 5G active antenna transmitter context," *IEEE Microwave Magazine*, vol. 20, no. 5, pp. 35–49, 2019.
- [21] Z. Niu, B. Zhang, J. Wang et al., "The research on 220 GHz multicarrier high-speed communication system," *China Communications*, vol. 17, no. 3, pp. 131–139, 2020.
- [22] Y. Zhou, L. Tian, C. Zhu et al., "Video coding optimization for virtual reality 360-degree source," *IEEE Journal of Selected Topics in Signal Processing*, vol. 14, no. 1, pp. 118–129, 2019.
- [23] W. Wang, N. Kumar, J. Chen et al., "Realizing the potential of the internet of things for smart tourism with 5G and AI," *IEEE Network*, vol. 34, no. 6, pp. 295–301, 2020.
- [24] J. Yang, J. Wen, B. Jiang, and H. Wang, "Blockchain-based sharing and tamper-proof framework of big data networking," *IEEE Network*, vol. 34, no. 4, pp. 62–67, 2020.
- [25] J. Wen, J. Yang, B. Jiang, H. Song, and H. Wang, "Big data driven marine environment information forecasting: a time series prediction network," *IEEE Transactions on Fuzzy Systems*, vol. 29, no. 1, pp. 4–18, 2021.